Svarva et al. 2019. Post print version.
Published in *Radiocarbon*, Vol 61, Nr 6, p 1765-1774

THE 1953–1965 RISE IN ATMOSPHERIC BOMB ^{14}C IN CENTRAL NORWAY

Helene Svarva, Pieter Grootes, Martin Seiler, Sølvi Stene, Terje Thun, Einar Værnes, and Marie-Josée Nadeau

Norwegian University of Science and Technology, NTNU University Museum – The National Laboratory for Age Determination, Sem Sælands vei 5, 7491 Trondheim, Norway

ABSTRACT. Sub-annual measurements, eight increments per year, of cellulose in a Scots pine tree growing in central Norway are presented as a proxy for tropospheric $^{14}CO_2$ at biweekly to monthly resolution. The results are validated by comparison to direct atmospheric measurements in the years 1959-1965, and a new dataset is obtained for 1953 to 1958. In this period, our cellulose measurements deviate from the Bomb 13 NH1 calibration curve, which is derived from single-year measurements of tree rings. This is due to seasonal cycles in tropospheric ^{14}C concentrations, caused by the first series of atmospheric nuclear weapons tests.

INTRODUCTION

Because carbon is fundamental to life, $^{14}CO_2$ has been given special attention among the radioactive tracers. Bomb radiocarbon is used in many applications, including studies of the carbon cycle and its dynamics, transport and reservoir exchange of CO_2 between the atmosphere, the oceans, and the biosphere (e.g. Nydal 1968; Oeschger et al. 1975; Broecker et al. 1980; Druffel and Suess 1983; Randerson et al. 2002; Hua and Barbetti 2007; Naegler and Levin 2009; Levin et al. 2010), dating of young material, and estimating regional fossil fuel CO_2 levels (e.g. Rakowski et al. 2004; Levin et al. 2011). This research relies on precise observations of atmospheric $^{14}CO_2$ that serve as a reference for the input into the carbon reservoirs.

The first regular measurements of the ^{14}C concentration of tropospheric CO_2 in the Northern Hemisphere revealed a clear seasonal cycle, superimposed on the general rise caused by the atmospheric nuclear weapons tests in the 1950s and 1960s (Nydal and Løvseth 1965; Nydal 1966; Levin et al. 1985; Levin and Kromer 2004). Prior to the Partial Test Ban Treaty in 1963, most bombs were detonated on the land surface or in the troposphere and the fireball was lifted into the stratosphere by thermal buoyancy, which then acted as a ^{14}C reservoir (Feely 1966; Bergkvist and Ferm 2000). $^{14}CO_2$ transferred down into the troposphere through the Northern Hemisphere spring exchange of air masses and consequently, the concentrations in the troposphere increased in spring and summer and decreased in autumn and winter (Nydal and Løvseth 1965; Nydal 1966).

However, these direct measurements of the ^{14}C concentration of atmospheric CO_2 started on a regular basis in 1959 in the Northern Hemisphere (Levin et al. 1985; Levin and Kromer 2004) and in December 1954 in the Southern Hemisphere (Manning et al. 1990), only after the first series of nuclear weapons tests had already raised tropospheric ^{14}C levels (Rafter and Fergusson 1957; Broecker and Walton 1959; Tauber 1960). Thus, the early part of the bomb calibration curve is based largely on single-year tree rings as a proxy for atmospheric ^{14}C

(Hua et al. 2013). But due to the seasonality in tree growth, ^{14}C concentrations in the cellulose of a full ring represent growth-weighted averages and will not capture the variability in atmospheric radiocarbon within a single year, especially when there are large and rapid changes in ^{14}C concentrations.

The stratosphere-troposphere mixing period coincides roughly with the growth period of trees at mid-latitude. Sub-annual sampling of single tree rings over the 1963 bomb peak have shown that the ^{14}C concentration of wood cellulose closely follows atmospheric ^{14}C concentrations (Grootes et al. 1989; Olsson and Possnert 1992; Cain et al. 2018). We present sub-annual ^{14}C measurements for the years 1953-1965, eight samples per year, obtained from a Scots pine tree (*Pinus sylvestris* L.) growing in central Norway. The results show the increase in bomb ^{14}C prior to the record of direct atmospheric measurements at biweekly to monthly resolution.

MATERIAL AND METHODS

Sample description

A Scots pine tree growing in Trøndelag, central Norway (63°16'27"N, 10°27'23"E, 134 m a.s.l.) was sampled from two directions with a 10 mm increment corer at breast height at the end of August 2017. At these latitudes, Scots pine has a clear annual ring structure and dark latewood that makes the ring boundaries visible. In this part of the stem, the tree has 86 annual rings, which were dated by ring counting. Ring widths for the period 1953 to 1965, all from the heartwood, range from 1.98 to 6.14 mm. One core was taken from the east side of the trunk, from which we sampled the rings from 1953 to 1965 and due to a narrow ring in 1957, two cores were taken from the west side, from which we sampled the rings from 1953 to 1956 and 1957 to 1965, respectively. The tree grows approximately 17 km south of the closest larger city (Trondheim) and is presumably not influenced by local fossil fuel effects. The surrounding forest was planted in the 1980s, and the canopy was open in the 1950s and 1960s. Mean annual temperature in this area was 2.7 °C between 1953 and 1965 and the mean annual precipitation sum in the same period was 958 mm (Norwegian Meteorological Institute, station code: 68860, 127 m a.s.l.).

Sample preparation and AMS ^{14}C analysis

The cores were incrementally sliced with a hand-held scalpel for the years 1953 to 1965, where the increment width was chosen to achieve eight slices per year resulting in a total of 208 samples. To remove oils, resin, and waxes, each sample was treated separately with petroleum ether for one hour. Then, the samples were pre-treated for ^{14}C analysis by extracting cellulose using an adaptation of the BABAB (base-acid-base-acid-bleach) protocol (Němec et al. 2010). First, the samples were treated with 4 % NaOH, followed by short steps of 4 % HCl, 4 % NaOH, and then 4 % HCl again at 75 °C. A bleaching step with a mixture of 5 % $NaClO_2$ and 4 % HCl at 75° C ($pH \leq 4$), with an ultrasonic bath at room temperature, follows at the end (Seiler et al. This issue). The resulting holocellulose was combusted in an elemental analyser, and the CO_2 was reduced to graphite with H_2 gas over a Fe catalyst in an

automated reduction system (Ohneiser 2006). Seiler et al. (This issue) describe the pre-treatment and graphitisation procedures in more detail.

The $^{14}C/^{12}C$ ratio and the $^{13}C/^{12}C$ ratio in the graphite were measured in the 1MV AMS system at the National Laboratory for Age Determination in Trondheim (Nadeau et al. 2015). Radiocarbon results are reported as $\Delta^{14}C$ (Δ of Stuiver and Polach 1977), which is calculated after correction for accelerator and preparation background, isotopic fractionation using $\delta^{13}C$ measurements from AMS, and the radioactive decay of sample and standards. The measurement uncertainties were calculated according to Nadeau and Grootes (2013) although the contributions from the fractionation correction and the normalisation to the standards were omitted as they are very small compared to the other uncertainties. The measurements were normalised to the Oxalic Acid II primary standards (NIST SRM-4990C, Mann 1983). The samples were measured in 15 different wheels together with other unknown samples as space permitted. Each wheel usually contains 10 (minimum eight) primary standards, five secondary standards, five process and machine blanks and 30 unknown samples. The blank correction was made assuming a modern contamination scaling inversely with the mass of the sample combusted (Seiler et al. This issue). The process blank curve was derived from measurements of coal samples of different weights measured over a few years as described by Seiler et al. (This issue).

Seventy-six targets (76) made from five different secondary standard materials were measured together with the samples in the various wheels: FIRI samples D, H, and J (Scott 2003), oxalic acid I (NIST SRM 4990 B), and IAEA-C7 (Le Clercq et al. 1997). These have a ^{14}C concentration ranging from 15 to 110 pMC. To compensate for the different radiocarbon concentrations and measurement uncertainties, the difference between measured and canonical values was normalised to the compounded uncertainty of the measurement and the canonical values (normalised deviation). The average of these should be centred around zero and the width of the distribution should be about 1 as it is in unit of σ. The average of the normalised deviations ($n = 76$) is 0.075 ± 0.11 σ indicating that there is no systematic offset. The standard deviation of the distribution is 1.07 σ indicating that the quoted uncertainties are representative of the true uncertainties of the measurements.

In addition, we measured the $^{13}C/^{12}C$ ratio of the cellulose in a Thermo Flash 2000 elemental analyser connected to a Thermo Delta V Advantage isotope-ratio mass spectrometer (IRMS). The results are reported relative to the VPDB standard. Due to unexpected results, samples from 1953 (increments 4, 8), 1954 (2), 1955 (1-8), 1956 (7, 8), 1962 (1-8), 1963 (1, 2), 1965 (1) of the west core were reduced and measured again. The weighted averages of these repeat measurements are presented, where the weights are the inversed square of the measurement uncertainty.

Timing of tree growth

Cumulative wood formation usually follows a sigmoid shape, with slow increment during spring and early summer, fast increment in midsummer, and decreasing activity towards the end of the vegetation period (e.g. Ford et al. 1978; Schmitt et al. 2004). In European and North American conifers of cold environments, the onset of cambial activity can vary from

the beginning of May to early June, depending on intra-annual weather-, snow-depth-, and soil conditions (Vaganov et al. 1999; Deslauriers et al. 2003; Rossi et al. 2007; Hettonen et al. 2009). Despite these variations, maximum growth rate seems to be limited to a short period, which in most European and North American conifer species is about the time of maximum day length (Rossi et al. 2006). Cessation of growth in Scots pine in Finland and Sweden usually takes place in August, depending on intra-annual conditions. In southern and northern Finland, wood formation ceased in mid-August (Mäkinen et al. 2008), and in Sweden, radial growth was found to cease in early- to mid-August (Andersson 1953). We combine measurements of the progress of the radial increment of Scots pine from the middle boreal and southern boreal zones in Finland over 15 and 18 years, respectively, between 1978 and 2007 from Hettonen et al. (2009). On average, 10% of the growth was completed by Julian date 162 ± 7, while 25%, 50%, 75%, and 90% were completed by Julian dates 173 ± 6, 185 ± 5, 200 ± 6, and 215 ± 9, respectively. Due to the increase in density associated with latewood formation in Scots pine, we do not adjust the timing of the sub-annual increments according to their mass as described by Cain et al. (2018). Assuming an onset of growth in mid-May and cessation of growth in mid-August, we thus interpolate a quadratic polynomial function from the data of Hettonen et al. (2009), and assign the eight sub-annual wood increments to midpoints at 29th May, 16th June, 21st June, 29th June, 7th July, 17th July, 27th July, and 9th August. Taking into account that there are differences between geographical regions in addition to the intra-annual variation, we estimate an uncertainty in assigning the sub-annual samples to a date of approximately two weeks, with a somewhat higher uncertainty for the first and last increments.

RESULTS AND DISCUSSION

Results of measurements and comparison to direct atmospheric ^{14}C measurements

Cellulose extraction yields were on average 68 % of the original sample mass with a range from 33-83 %, and cellulose carbon contents were on average 44 %, with an a range from 34-52 %. We find no seasonal cycle in cellulose extraction yields or carbon content for the measured samples, however, cellulose extraction yields are on average 7 % lower for the east core than for the west cores, with minimum values on the east core in 1959. The lowered cellulose yields are not associated with reduced carbon content or very narrow rings. The variation in extraction yields might thus be a result of variations in wood composition, in addition to weighing imprecision and/or humidity. This might also explain the variation in carbon content, although these are smaller than for the cellulose yields.

Due to the uncertainty associated with the assignment of a certain growing period to each sub-annual increment, attempts were made to fit the IRMS $\delta^{13}C$ results to the record of atmospheric $\delta^{13}C$ measurements in the Northern Hemisphere. This record features two main trends. Firstly, a seasonal cycle occurs with an increase in the $^{13}C/^{12}C$ ratio during summer when the selective assimilation of the light isotope during plant photosynthesis exceeds the remineralisation of older plant material, and a decrease in winter with reduced or halted photosynthesis and increased fossil fuel combustion (e.g. Mook et al. 1983). Secondly, a long-term decrease with time occurs with the increase in combustion of fossil fuels (Keeling 1979).

We compared our IRMS $\delta^{13}C$ results to the seasonal cycle in atmospheric $\delta^{13}C$ measurements from Point Barrow, Alaska between 1983 and 2008 (Keeling et al. 2010), corrected for the inter-annual trend associated with fossil fuel combustion by assuming a linear decrease in monthly averages. However, the IRMS $\delta^{13}C$ values of our tree show an irregular, larger seasonal amplitude than the Point Barrow atmospheric measurements. We interpret this as the $\delta^{13}C$ signal in the tree being not only dependent on the atmospheric ratio, but also on other environmental factors, making our $\delta^{13}C$ IRMS measurements unsuited for adjusting the timing of the growing season.

We repeated 24 samples of the west core to check reproducibility and some apparently aberrant results. The average difference between original $\Delta^{14}C$ measurement and repeat should ideally equate zero. Instead, we get an average offset from zero of 8.4 ‰ with a standard deviation of 16.1 ‰, much larger than the 3.4 ‰ expected from our measurement uncertainty. When disregarding deviating measurements between the two cores in the first and last increments, which might be influenced by wood from the previous or following year, the average offset is 2.8 ‰ with a standard deviation of 9.8 ‰ over 16 samples with repeats. This is not significantly different from zero and the standard deviation is closer to the combined one sigma measurement uncertainty for the differences, which range from 2.3 to 4.8 ‰ for the 16-sample set. Further exclusion of increments from years when the increase in atmospheric ^{14}C was steep (1962, 63) yields an average offset of 0.8 ‰ and a standard deviation of 5.8 ‰ over 11 samples with repeats. This indicates that poor reproduction of repeats stems mostly from inhomogeneities in the cellulose, connected to the difficulty of exactly finding the boundaries for each annual ring in the manual sectioning of the wood core and to rapidly increasing atmospheric ^{14}C levels during the growing season.

The east and west cores show the same general trend, but with some discrepancies between the cores, which mainly occur in the first and last increments of a year (Supplementary Figure S1 and Table S1). Such deviating measurements, visually identified, occur in the west cores in 1958 (increment 8), 1959 (1), 1960 (1), 1962 (1, 2), and in 1965 (1) and in the east core in 1956 (1, 8), 1957 (1), 1958 (7,8), 1959 (8), 1961 (8), 1962 (8), 1964 (8), and 1965 (8). These could be explained by having some wood of the previous or next year in the sample due to inaccuracies in the manual sectioning. All the deviating measurements are retained in Figure 1 and 2 and in the supplementary material because, in years with rapidly increasing or decreasing ^{14}C content, such deviations could reflect real atmospheric changes. There are also discrepancies between the east and west cores in 1962 (4, 5), which might be caused by cellulose ^{14}C inhomogeneity due to rapidly increasing atmospheric levels (Supplementary Figure S1).

The sub-annual cellulose ^{14}C measurements of both cores in the period 1959-1965 are compared to direct atmospheric $\Delta^{14}C$ measurement values from stations in Vermunt, Austria (Levin et al. 1985; Levin and Kromer 2004), Abisko, Sweden (Olsson and Karlén 1965; Stenberg and Olsson 1967; Olsson and Klasson 1970), Kapp Linné on Spitsbergen (Olsson and Karlén 1965; Stenberg and Olsson 1967; Olsson and Klasson 1970; Nydal and Løvseth 1983), and in Norway (Nydal and Løvseth 1983) in Figure 1. The highest cellulose $\Delta^{14}C$ value (933.7 ± 3.3 ‰) was measured for increment number seven of the east core in 1964,

which was assigned to the 27th July midpoint. Tropospheric $\Delta^{14}C$ levels were higher in 1963, however, the 1963 peak was not reached until late August (Nydal and Løvseth 1983) or in September (Olsson and Karlén 1965), after the cessation of growth.

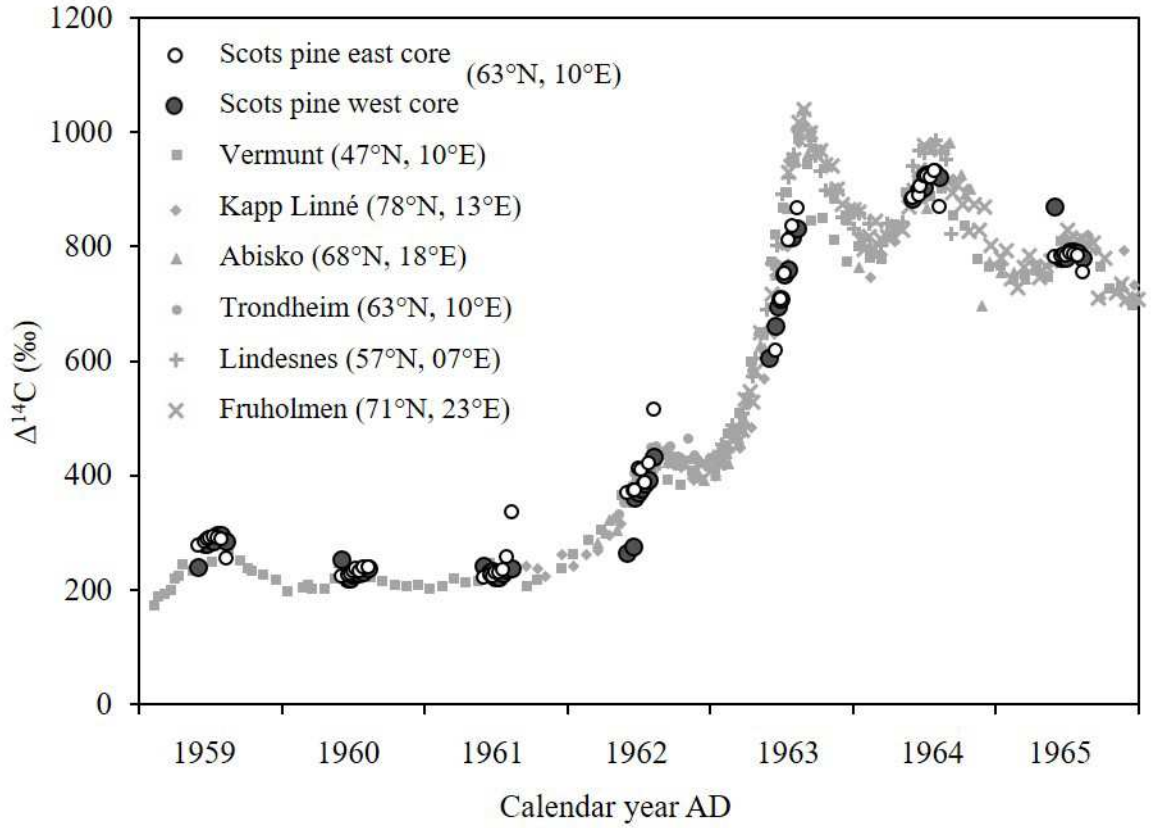

Figure 1: Sub-annual cellulose $\Delta^{14}C$ values in two wood cores from a Scots pine from central Norway for the years 1959 to 1965, compared to direct measurements of atmospheric $\Delta^{14}C$ from Vermunt in Austria (Levin et al. 1985; Levin and Kromer 2004), Kapp Linné on Spitsbergen (Olsson and Karlén 1965; Stenberg and Olsson 1967; Olsson and Klasson 1970; Nydal and Løvseth 1983), Abisko in northern Sweden (Olsson and Karlén 1965; Stenberg and Olsson 1967; Olsson and Klasson 1970), Trondheim in central Norway (Nydal and Løvseth 1983), Lindesnes in southern Norway (Nydal and Løvseth 1983), and Fruholmen in northern Norway (Nydal and Løvseth 1983). Error bars are too small to show in the figure.

Our Scots pine $\Delta^{14}C$ values, disregarding the measurements that deviates between the cores, mimic the direct atmospheric measurements from Vermunt for the years 1959 through 1965, except for 1963, where they are lower. In 1963, we observe an apparent parallel shift of about a month in our Scots pine compared to atmospheric measurements (Supplementary Figure S2). A similar shift was observed by Grootes et al. (1989) and Cain et al. (2018) and was attributed to a contribution of 13 % to 28 % of soil CO_2 from decomposing plant material of previous years and to atmospheric circulation patterns, respectively. When comparing the

atmospheric ^{14}C records of different latitudes in the Northern Hemisphere, we note that Abisko in northern Sweden and Kapp Linné on Spitsbergen increases later in 1963 than records from Vermunt and Lindesnes. This could be because of increasing distance from the area of stratospheric injection into the troposphere although the results from Fruholmen, at a latitude that of between Kapp Linné and Abisko, do not show this delay. Values for Trondheim in May, June and July of 1963 are missing and more research is needed to investigate whether the apparent delay in cellulose $\Delta^{14}C$ values compared to the atmosphere is due to the tree's use of stored photosynthates, growth period changes, soil CO_2, or some other mechanism that results in an apparent reservoir effect.

Cellulose $\Delta^{14}C$ values between 1953 and 1958

Our measurements in 1954, 1956, 1957, and 1958 (Figure 2) clearly deviate from the Bomb 13 NH1 calibration curve (Hua et al. 2013). The bomb curve interpolates an even increase in $\Delta^{14}C$ values between 1956 and 1959 based on full ring values, while our Scots pine ^{14}C measurements show a clear seasonal signal in this period, analogous to that observed in the years 1959 to 1965. This is especially pronounced from 1955, following the heavy bomb tests in the summer of 1954. The growing season in Trondheim starts later and ends earlier than at mid-latitude. This may explain some of the differences between our measurements and the calibration curve. This is clearly seen in 1963, when the Trondheim tree does not reach the atmospheric peak. In 1958, the Trondheim tree suggests an increase of 78.6 ‰ in $\Delta^{14}C$ values based on a weighted average of the two cores from May to August, which is just as steep as the increase in 1959. This is probably caused by nuclear tests amounting to 6.4 Mt (megaton TNT equivalent) being detonated in the fall of 1957, together with a larger proportion of nuclear tests being carried out at high latitudes early in the growing season of 1958 compared to previous years. The yield of detonations between January and March of 1958 on test sites in East Kazakhstan (50°N, 78°E) and on Novaya Zemlya (74°N, 56°E) amounted to a total of 3.38 Mt (Bergkvist and Ferm 2000). These explosions may have contributed to raising tropospheric ^{14}C levels in central Norway in the growing season in the same year. This might also explain why our cellulose $\Delta^{14}C$ levels are higher than Vermunt atmosphere in 1959. In 1954, when annual detonation yield was over 48 Mt, we only observe a 7.9 ‰ increase in the cellulose $\Delta^{14}C$ values. Although the largest bombs were detonated between January and May of 1954, these tests were carried out on the Bikini (11°N, 165°E) and Enewetak (11°N, 162°E) atolls in the tropical Pacific Ocean. ^{14}C created from these explosions does not seem to have reached central Norway until the atmospheric mixing in the spring of 1955.

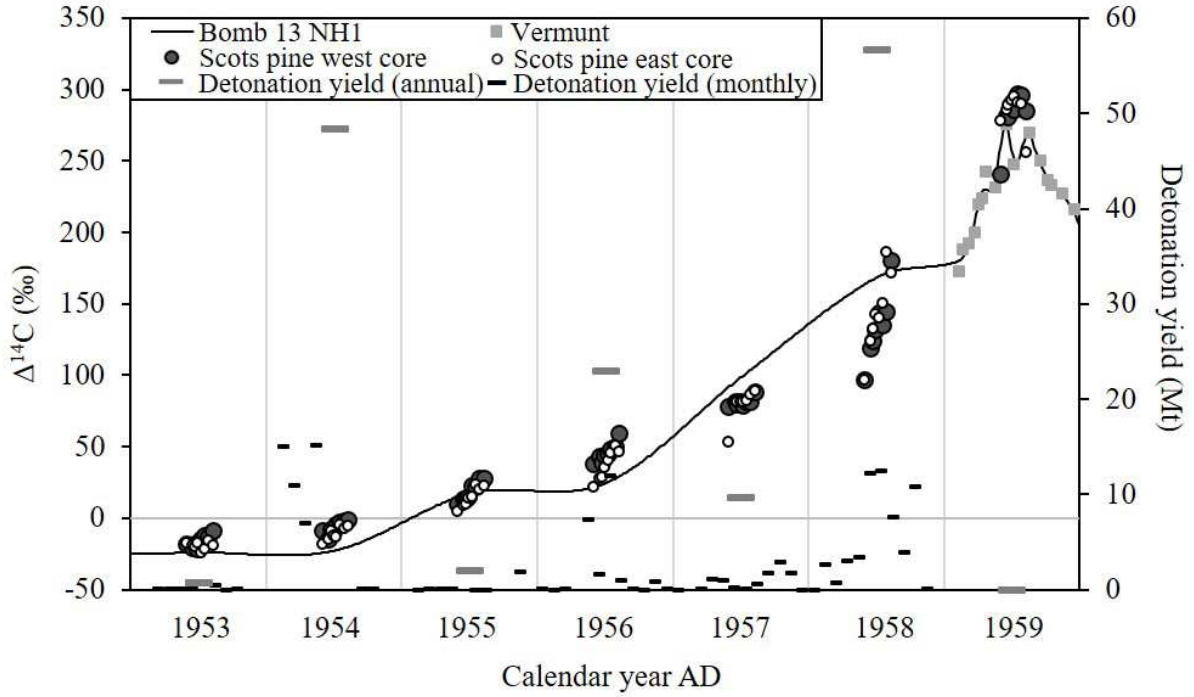

Figure 2: Sub-annual cellulose $\Delta^{14}C$ values in a Scots pine from central Norway (63°N, 10°E) for the years 1953 to 1959, compared to direct measurements of atmospheric $\Delta^{14}C$ from Vermunt (47°N, 10°E) in Austria (1959 only; Levin et al. 1985; Levin and Kromer 2004), the Bomb 13 NH1 calibration curve (Hua et al. 2013), and to monthly and annual detonation yields (Mt) from aboveground nuclear weapons tests (Bergkvist and Ferm 2000). Error bars are too small to show in the figure.

Sub-annual tree-ring measurements as a tracer for atmospheric ^{14}C

Because most atmospheric nuclear weapons tests were carried out in the Northern Hemisphere, large ^{14}C gradients were observed in the troposphere in the 1960s (Nydal 1966). Intra- and interhemispheric differences in ^{14}C concentrations have also been shown to be modified by atmospheric circulation and ocean uptake in this period (e.g. Randerson et al. 2002; Hua and Barbetti 2007). Therefore, to quantify the immediate atmospheric ^{14}C response to nuclear tests carried out in the 1950s and complete the record of atmospheric radiocarbon for the period 1950-2010 (Hua et al. 2013), our measurements of the ^{14}C concentrations in the Trondheim pine should be repeated by sub-annual sampling of tree rings at different latitudes and longitudes.

Recent research has emphasised the significance of rapid excursions in atmospheric ^{14}C concentration (Miyake et al. 2012; 2013) and the limitations of decadally averaged calibration data (Bayliss et al. 2017), which again has prompted researchers around the world to create and apply more detailed datasets (e.g. Wacker et al. 2014; Sigl et al. 2015; Dee and Pope 2016; Pearson et al. 2018). However, comparisons of the ^{14}C concentration in the earlywood contra latewood of certain deciduous tree species have revealed that efforts to produce single-

year calibration curves need to take into account the intra-seasonal variability in tree rings and the differences in the deposition of stored carbon in different species of trees (McDonald et al. 2018). We here confirm the findings of Grootes et al. (1989) that coniferous trees grown in open conditions can be excellent proxies for atmospheric $^{14}CO_2$, even on a sub-annual basis. Our results show that in periods of rapid changes in atmospheric ^{14}C concentrations, measuring only the earlywood and latewood is insufficient to utilise the potential for obtaining the full details on atmospheric change that is available in tree rings.

CONCLUSIONS

Sub-annual sampling of Scots pine tree rings in central Norway over the 1959-1965 bomb peak confirms earlier findings that tree cellulose can trace the changes in atmospheric ^{14}C content at a biweekly to monthly resolution. A new dataset for the period 1953 to 1958, reveals a seasonal signal in atmospheric ^{14}C before the onset of direct atmospheric measurements in 1959 and a detailed response of the atmospheric ^{14}C concentration in central Norway to the aboveground nuclear weapons tests in this period. Accurate knowledge of the timing of the tree's radial growth and of its potential use of stored photosynthate or sub-canopy air is needed to fully utilise the sub-annual information in tree rings.

ACKNOWLEDGEMENTS

We thank the Norwegian University of Science and Technology and especially its University Museum for their support. Thank you also to two reviewers whose comments helped improve the manuscript.

REFERENCES

Andersson S-O. 1953. Om tidpunkten för den årliga diametertillväxtens avslutande hos tall och gran. *Meddelanden från Statens Skogsforskningsinstitut* 43(5): 27p.

Bayliss A, Marshall P, Tyers C, Bronk Ramsey C, Cook G, Freeman SPHT, Griffiths S. 2017. Informing conservation: towards ^{14}C wiggle-matching of short tree-ring sequences from medieval buildings in England. *Radiocarbon* 59(3): 985-1007.

Bergkvist N-O, Ferm R. 2000. *Nuclear explosions 1945-1998*. FAO-Stockholm International Peace Research Institute. User Report. Stockholm. 42p.

Broecker WS, Walton A. 1959. Radiocarbon from nuclear tests. *Science* 130(3371): 309-14.

Broecker WS, Peng T-H, Engh R. 1980. Modeling the carbon system. *Radiocarbon* 22(3): 565-98.

Cain WF, Griffin S, Druffel-Rodriguez KC, Druffel ERM. 2018. Uptake of carbon for cellulose production in a white oak from western Oregon, USA. *Radiocarbon* 60(1): 151-58.

Dee MW, Pope BJS. 2016. Anchoring historical sequences using a new source of astro-chronological tie-points. *Proceedings of the Royal Society A* 472: 20160263, doi:10.1098/rspa.2016.0263.

Deslauriers A, Morin H, Urbinati C, Carrer M. 2003. Daily weather response of balsam fir (*Abies balsamea* (L.) Mill.) stem radius increment from dendrometer analysis in the boreal forest of Québec (Canada). *Trees* 17: 477-84.

Druffel E, Suess HE. 1983. On the radiocarbon record in banded corals: exchange parameters and net transport of $^{14}CO_2$ between atmosphere and surface ocean. *Journal of Geophysical Research* 88(C2): 1271-80.

Feely HW, Seitz H, Lagomarsino RJ, Biscaye PE. 1966. Transport and fallout of stratospheric radioactive debris. *Tellus* 18(2): 316-28.

Ford ED, Robards AW, Piney MD. 1978. Influence of environmental factors in cell production and differentiation on the early wood of *Picea sitchensis*. *Annals of Botany* 42(3): 683-92.

Grootes PM, Farwell GW, Schmidt FH, Leach DD, Stuiver M. 1989. Rapid response of tree cellulose radiocarbon content to changes in atmospheric $^{14}CO_2$ concentration. *Tellus* 41B: 134-48.

Hettonen HM, Mäkinen H, Nöjd P. 2009. Seasonal dynamics of the radial increment of Scots pine and Norway spruce in the southern and middle boreal zones of Finland. *Canadian Journal of Forest Research* 39: 606-18.

Hua Q, Barbetti M. 2007. Influence of atmospheric circulation on regional $^{14}CO_2$ differences. *Journal of Geophysical Research* 112: D19102, doi:10.1029/ 2006JD007898.

Hua Q, Barbetti M, Rakowski AZ. 2013. Atmospheric radiocarbon for the period 1950-2010. *Radiocarbon* 55(4): 2059-72.

Keeling CF. 1979. The Suess effect: ^{13}carbon-^{14}carbon interrelations. *Environment International* 2: 229-300.

Keeling RF, Piper SC, Bollenbacher AF, Walker SJ. 2010. Monthly atmospheric $^{13}C/^{12}C$ isotopic ratios for 11 SIO stations. In Trends: a compendium of data on global change. Carbon Dioxide Information Analysis Center, Oak ridge National Laboratory, US Department of Energy, Oak Ridge, Tenn., USA. http://cdiac.ess-dive.lbl.gov/trends/co2/iso-sio/iso-sio.html.

Le Clercq M, van der Plicht J, Gröning M. 1997. New ^{14}C reference materials with activities of 15 and 50 pMC. *Radiocarbon* 40(1): 295-97.

Levin I, Hammer S, Eichelmann E, Vogel FR. 2011. Verification of greenhouse gas emission reductions: the prospect of atmospheric monitoring in polluted areas. *Philosophical Transactions of the Royal Society A* 369: 1906-24.

Levin I, Kromer B. 2004. The tropospheric $^{14}CO_2$ level in mid-latitudes of the Northern Hemisphere (1959-2003). *Radiocarbon* 46(3): 1261-72.

Levin I, Kromer B, Schoch-Fischer H, Bruns M, Münnich M, Berdau D, Vogel JC, Münnich KO. 1985. 25 years of tropospheric ^{14}C observations in central Europe. *Radiocarbon* 27(1): 1-19.

Levin I, Naegler T, Kromer B, Diehl M, Francey RJ, Gomez-Pelaez AJ, Steele P, Wagenbach D, Weller R, Worthy DE. 2010. Observations and modelling of the global distribution and long-term trend of atmospheric $^{14}CO_2$. *Tellus* 62B: 26-46.

McDonald L, Chivall D, Miles D, Bronk Ramsey C. 2018. Seasonal variations in the ^{14}C content of tree rings: influences on radiocarbon calibration and single-year curve construction. *Radiocarbon* 61(1): 185-94.

Mäkinen H, Seo J-W, Nöjd P, Schmitt U, Jalkanen R. 2008. Seasonal dynamics of wood formation: a comparison between pinning, microcoring and dendrometer measurements. *European Journal of Forest Research* 127: 235-45.

Mann WB. 1983. An international reference material for radiocarbon dating*. *Radiocarbon* 25(2): 519-27.

Manning MR, Lowe DC, Melhuish WH, Sparks RJ, Wallace G, Brenninkmeijer CAM, McGill RC. 1990. The use of radiocarbon measurements in atmospheric studies. *Radiocarbon* 32(1): 37-58.

Miyake F, Masuda K, Nakamura T. 2013. Another rapid event in the carbon-14 content of tree rings. *Nature Communications* 4: 1748.

Miyake F, Nagaya K, Masuda K, Nakamura T. 2012. A signature of cosmic-ray increase in AD 774-775 from tree rings in Japan. *Nature* 486: 240-42.

Mook WG, Koopmans M, Carter AF, Keeling CF. 1983. Seasonal, latitudinal, and secular variations in the abundance and isotopic ratios of atmospheric carbon dioxide 1. results from land stations. *Journal of Geophysical Research* 88(C15): 10915-33.

Nadeau M-J, Grootes PM. 2013. Calculation of the compounded uncertainty of ^{14}C AMS measurements. *Nuclear Instruments and Methods in Physics Research B* 294: 420-25.

Nadeau M-J, Værnes E, Svarva HL, Larsen E, Gulliksen S, Klein M, Mous DJW. 2015. Status of the “new” AMS facility in Trondheim. *Nuclear Instruments and Methods in Physics Research* 361B: 149-55.

Naegler T, Levin I. 2009. Biosphere-atmosphere gross carbon exchange flux and the $\delta^{13}CO_2$ and $\Delta^{14}CO_2$ disequilibria constrained by the biospheric excess radiocarbon inventory. *Journal of Geophysical Research* 114: D17303, doi:10.1029/2008JD011116.

Němec M, Wacker L, Hajdas I, Gäggeler H. 2010. Alternative methods for cellulose preparation for AMS measurement. *Radiocarbon* 52(2-3): 1358-70.

Nydal R. 1966. Variation in C^{14} concentration in the atmosphere during the last several years. *Tellus* 18(2): 271-79.

Nydal R, Løvseth K. 1965. Distribution of radiocarbon from nuclear tests. *Nature* 206(4988): 1029-31.

Nydal R, Løvseth K. 1983. Tracing bomb ^{14}C in the atmosphere 1962-1980. *Journal of Geophysical Research* 88(C6): 3621-42.

Nydal R. 1968. Further investigation on the transfer of radiocarbon in nature. *Journal of Geophysical Research* 73(12): 3617-35.

Oeschger H, Siegenthaler U, Schotterer U, Gugelmann A. 1975. A box diffusion model to study the carbon dioxide exchange in nature. *Tellus* 27(2): 168-92.

Ohneiser A. 2006. Entwicklung einer automatischen CO_2-Reduktionsanlage zur Probenvorbereitung am AMS Radiokarbonlabor Erlangen. Thesis, Friedrich-Alexander-Universität Erlangen-Nürnberg.

Olsson IU, Karlén I. 1965. Uppsala radiocarbon measurements VI. *Radiocarbon* 7: 331-35.

Olsson IU, Klasson M. 1970. Uppsala radiocarbon measurements X. *Radiocarbon* 12(1): 281-84.

Olsson I, Possnert G. 1992. ^{14}C activity in different sections and chemical fractions of oak tree rings, AD 1938-1981. *Radiocarbon* 34(3): 757-67.

Pearson CL, Brewer PW, Brown D, Heaton TJ, Hodgins GWL, Jull AJT, Lange T, Salzer MW. 2018. Annual radiocarbon record indicates 16th century BCE date for the Thera eruption. *Science Advances* 4: eaar8241.

Rafter TA, Fergusson GJ. 1957. "Atom bomb effect"—Recent increase of carbon-14 content of the atmosphere and biosphere. *Science* 126(3273): 557-58.

Rakowski A, Kuc T, Nakamura T, Pazdur A. 2004. Radiocarbon concentration in the atmosphere and modern tree rings in the Kraków area, southern Poland. *Radiocarbon* 46(2): 911-16.

Randerson JT, Enting IG, Schuur EAG, Caldeira K, Fung IY. 2002. Seasonal and latitudinal variability of troposphere $\Delta^{14}CO_2$: post bomb contributions from fossil fuels, oceans, the stratosphere, and the terrestrial biosphere. *Global Geochemical Cycles* 16(4): doi:10.1029/2002GB001876.

Rossi S, Deslauriers A, Anfodillo T, Carraro V. 2007. Evidence of threshold temperatures for xylogenesis in conifers at high altitudes. *Oecologia* 152: 1-12.

Rossi S, Deslauriers A, Anfodillo T, Morin H, Saracino A, Motta R, Borghetti M. 2006. Conifers in cold environments synchronize maximum growth rate of tree-ring formation with day length. *New Phytologist* 170: 301-10.

Schmitt U, Jalkanen R, Eckstein D. 2004. Cambium dynamics of *Pinus sylvestris* and *Betula* spp. in the northern boreal forest in Finland. *Silva Fennica* 38(2): 167-78.

Scott EM. 2003. Section 2: the results. *Radiocarbon* 45(2): 151-57.

Seiler M, Grootes PM, Haarsaker J, Lélu S, Rzadecka-Juga I, Stene S, Svarva HL, Thun T, Værnes E, Nadeau M-J. (This issue). Status report of the Trondheim AMS radiocarbon laboratory. *Radiocarbon* (Accepted with minor revision)

Sigl M, Winstrup M, McConnell JR, Welten KC, Plunkett G, Ludlow F, Büntgen U, Caffee M, Chellman N, Dahl-Jensen D, Fischer H, Kipfstuhl S, Kostick C, Maselli OJ, Mekhaldi F, Mulvaney R, Muscheler R, Pasteris DR, Pilcher JR, Salzer M, Schüpbach S, Steffensen JP, Vinther BM, Woodruff TE. 2015. Timing and climate forcing of volcanic eruptions for the past 2,500 years. *Nature* 523: 543-49.

Stenberg A, Olsson IU. 1967. Uppsala radiocarbon measurements VIII. *Radiocarbon* 9: 471-76.

Stuiver M, Polach HA. 1977. Discussion: reporting of ^{14}C data. *Radiocarbon* 19(3): 355-63.

Tauber H. 1960. Post-bomb rise in radiocarbon activity in Denmark. *Science* 131(3404): 921-22.

Vaganov EA, Hughes MK, Kirdyanov AV, Schweingruber FH, Silkin PP. 1999. Influence of snowfall and melt timing on tree growth in subarctic Eurasia. *Nature* 400: 149-51.

Wacker L, Güttler D, Goll J, Hurni JP, Synal H-A, Walti N. 2014. Radiocarbon dating to a single year by means of rapid atmospheric ^{14}C changes. *Radiocarbon* 56(2): 573-79.

451

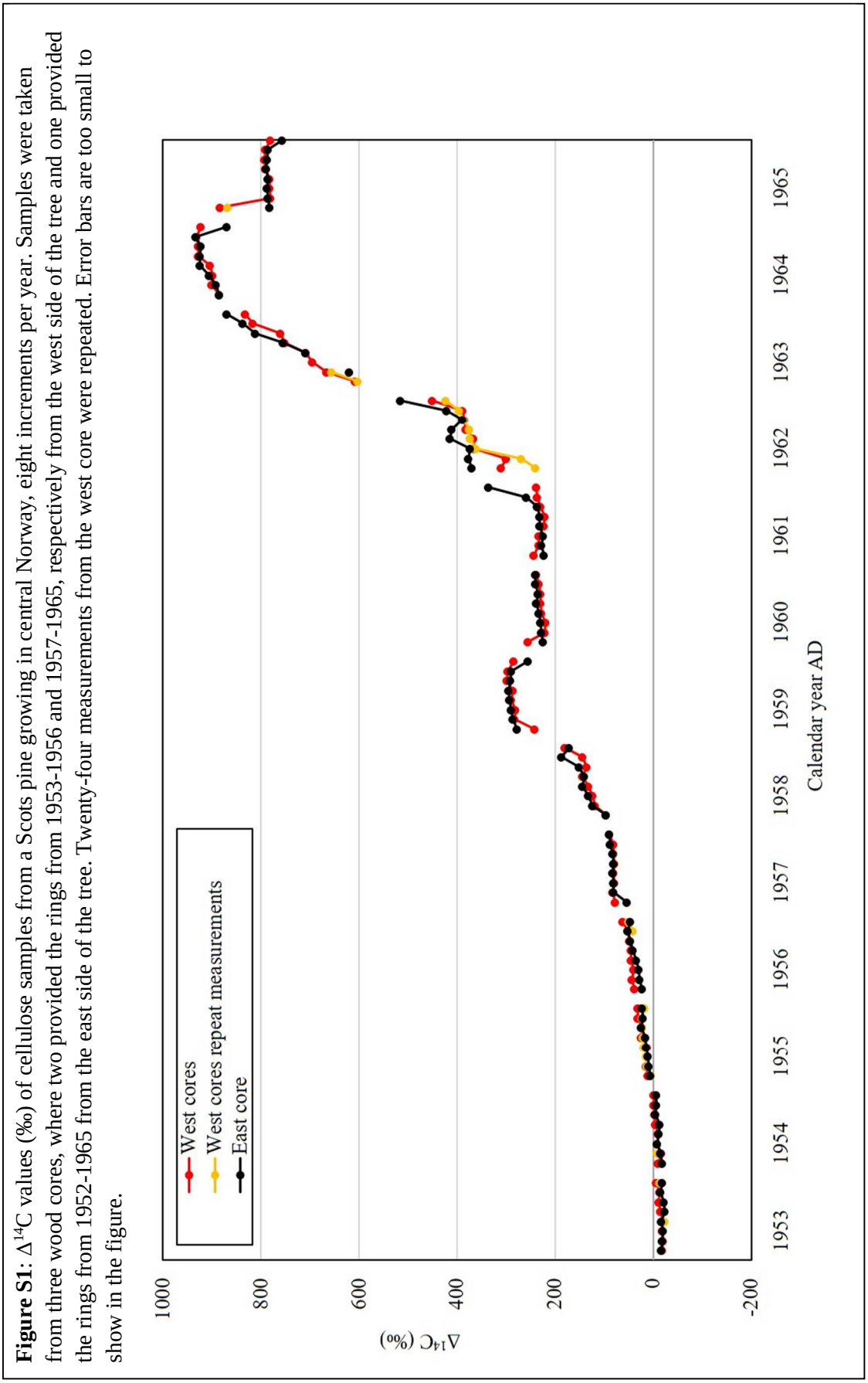

Figure S1: $\Delta^{14}C$ values (‰) of cellulose samples from a Scots pine growing in central Norway, eight increments per year. Samples were taken from three wood cores, where two provided the rings from 1953-1956 and 1957-1965, respectively from the west side of the tree and one provided the rings from 1952-1965 from the east side of the tree. Twenty-four measurements from the west core were repeated. Error bars are too small to show in the figure.

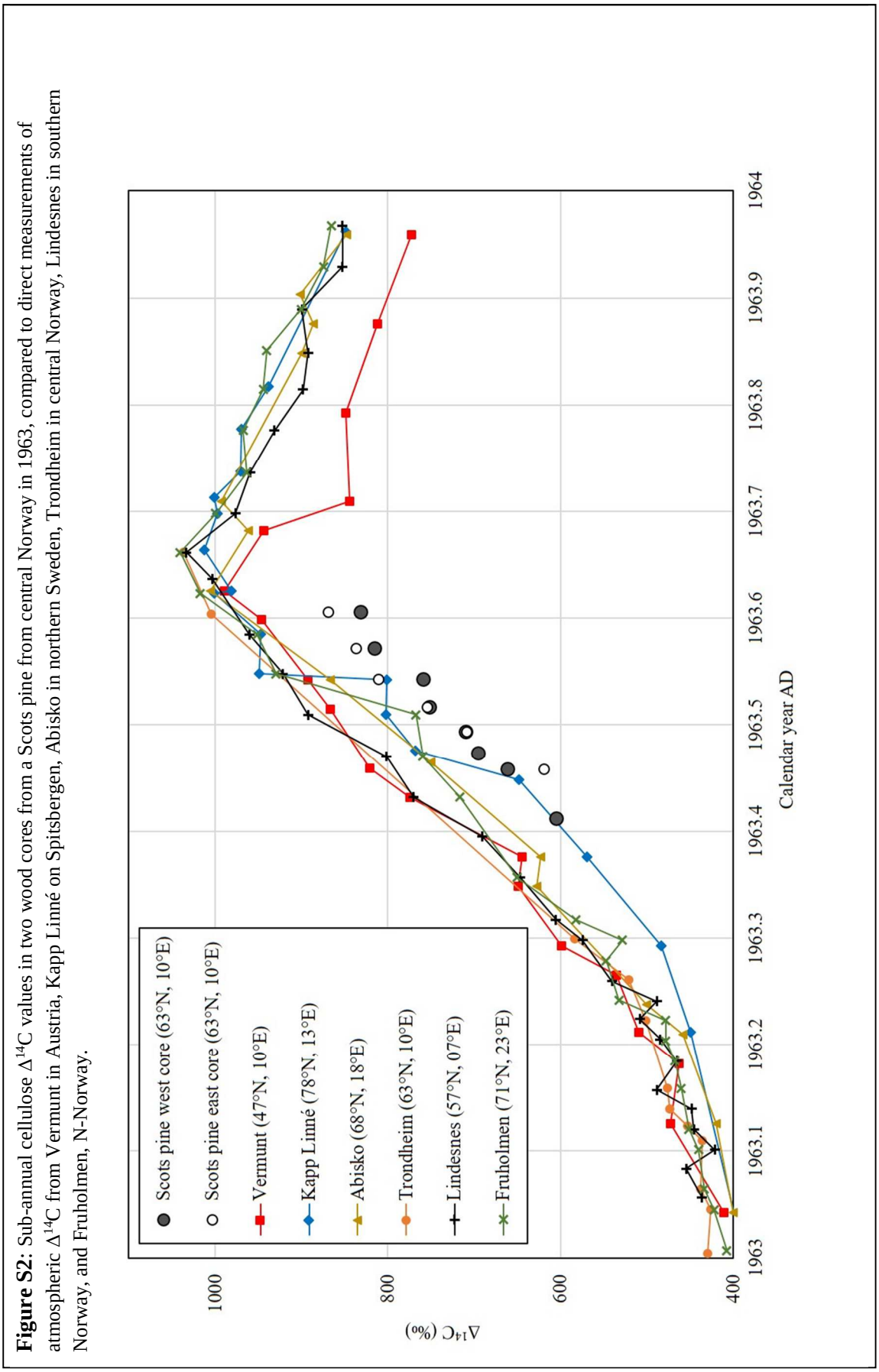

Figure S2: Sub-annual cellulose $\Delta^{14}C$ values in two wood cores from a Scots pine from central Norway in 1963, compared to direct measurements of atmospheric $\Delta^{14}C$ from Vermunt in Austria, Kapp Linné on Spitsbergen, Abisko in northern Sweden, Trondheim in central Norway, Lindesnes in southern Norway, and Fruholmen, N-Norway.

452

Table S1: Radiocarbon measurements of sub-annual increments of Scots pine cored from the east and the west side over the years 1953 to 1965. Timing of growth (Year AD), lab ID (TRa-#), number of AMS measurements (n), $\Delta^{14}C$ values (‰), measurement error (± ‰), and $\delta^{13}C$ values (‰) from IRMS. Discrepancies between the cores that are mentioned in the text and presumed to stem from inaccuracies in the sectioning are marked with an asterisk next to the number of AMS measurements.

Cellulose midpoint	West cores					East core				
Year (AD)	TRa #	n	$\Delta^{14}C$ (‰)	± (‰)	$\delta^{13}C$ (‰)	TRa #	n	$\Delta^{14}C$ (‰)	± (‰)	$\delta^{13}C$ (‰)
1953.41	12762	1	-17.7	1.1	-25.7	13487	1	-17.1	2.4	-25.2
1953.46	12763	1	-20.4	1.4	-24.5	13488	1	-19.1	3.1	-26.1
1953.47	12764	1	-18.0	1.8	-24.5	13489	1	-19.9	2.8	-25.6
1953.49	12765	2	-21.3	2.8	-24.2	13490	1	-17.1	2.4	-24.8
1953.52	12766	1	-14.7	1.5	-24.3	13491	1	-24.3	2.8	-24.6
1953.54	12767	1	-11.7	1.8	-24.4	13492	1	-21.1	2.7	-24.3
1953.57	12768	1	-12.5	1.3	-24.4	13493	1	-15.1	2.4	-24.1
1953.61	12769	2	-8.8	3.0	-24.3	13494	1	-19.1	2.6	-24.0
1954.41	12770	1	-9.0	1.3	-26.1	13495	1	-18.0	2.7	-24.7
1954.46	12771	2	-14.3	2.6	-26.0	13496	1	-14.3	2.5	-24.6
1954.47	12772	1	-8.1	1.5	-25.9	13497	1	-8.9	2.6	-24.9
1954.49	12773	1	-9.8	1.4	-25.0	13498	1	-12.0	2.4	-24.7
1954.52	12774	1	-4.0	1.6	-24.9	13499	1	-13.1	2.4	-24.3
1954.54	12775	1	-2.3	1.3	-25.6	13500	1	-4.4	2.3	-24.2
1954.57	12776	1	-1.5	1.3	-25.7	13501	1	-6.5	2.2	-24.5
1954.61	12777	1	-1.3	1.5	-25.5	13502	1	-5.6	2.1	-24.8
1955.41	12778	2	9.9	2.7	-26.1	13503	1	4.8	2.3	-25.2
1955.46	12779	2	13.6	2.5	-25.9	13504	1	9.5	2.9	-24.7
1955.47	12780	2	13.4	2.5	-	13505	1	10.4	2.1	-24.8
1955.49	12781	2	15.1	2.5	-	13506	1	14.5	2.2	-24.9
1955.52	12782	2	23.0	2.9	-26.2	13507	1	15.4	2.8	-24.9
1955.54	12783	2	22.5	2.6	-25.4	13508	1	24.2	2.5	-25.0
1955.57	12784	2	28.3	2.3	-25.4	13509	1	20.3	2.2	-24.5
1955.61	12785	2	28.1	3.2	-25.6	13510	1	22.8	2.5	-24.1
1956.41	12786	1	38.3	1.6	-26.2	13511	1*	21.9	2.2	-23.3
1956.46	12787	1	43.5	1.6	-26.0	13512	1	28.6	2.3	-24.2
1956.47	12788	1	39.3	1.7	-25.6	13513	1	28.8	2.3	-25.2
1956.49	12789	1	44.2	1.9	-25.2	13514	1	35.4	2.2	-24.7
1956.52	12790	1	45.0	1.3	-25.1	13515	1	40.9	3.1	-25.1
1956.54	12791	1	48.2	1.3	-24.7	13516	1	46.2	2.9	-24.7
1956.57	12792	2	49.9	3.1	-25.2	13517	1	51.2	2.5	-24.8
1956.61	12793	2	59.9	3.0	-25.5	13518	1*	46.7	2.8	-

460

461

462 *Table S1 continued.*

Cellulose midpoint	West cores					East core				
Year (AD)	TRa #	n	$\Delta^{14}C$ (‰)	± (‰)	$\delta^{13}C$ (‰)	TRa #	n	$\Delta^{14}C$ (‰)	± (‰)	$\delta^{13}C$ (‰)
1957.41	13081	1	78.0	2.6	-25.0	13519	1*	53.2	2.3	-24.8
1957.46	13082	1	81.8	2.6	-25.1	13520	1	81.3	2.3	-25.7
1957.47	13083	1	79.9	2.5	-24.8	13521	1	81.4	2.5	-24.9
1957.49	13084	1	81.3	2.6	-24.6	13522	1	82.1	2.4	-24.6
1957.52	13085	1	79.2	2.7	-24.3	13523	1	81.5	2.4	-24.7
1957.54	13086	1	81.4	2.6	-24.3	13524	1	82.3	2.2	-24.1
1957.57	13087	1	81.6	2.7	-24.3	13525	1	87.1	2.2	-24.4
1957.61	13088	1	88.9	2.6	-24.7	13526	1	89.2	2.2	-24.4
1958.41	13089	1	96.6	2.7	-25.5	13527	1	97.0	1.9	-25.2
1958.46	13090	1	119.0	2.7	-25.6	13528	1	124.0	2.2	-25.2
1958.47	13091	1	124.0	2.6	-25.8	13529	1	132.6	2.0	-25.0
1958.49	13092	1	131.9	2.9	-25.2	13530	1	143.4	2.3	-24.7
1958.52	13093	1	144.2	2.7	-25.5	13531	1	140.4	2.3	-24.7
1958.54	13094	1	135.1	2.9	-25.7	13532	1	150.3	2.4	-25.3
1958.57	13095	1	144.9	2.7	-25.7	13533	1*	186.6	1.9	-25.0
1958.61	13096	1*	180.3	2.7	-25.1	13534	1*	171.8	2.4	-25.1
1959.41	13097	1*	241.3	2.8	-25.9	13535	1	278.4	2.8	-24.8
1959.46	13098	1	282.0	2.8	-25.6	13536	1	286.2	2.8	-24.7
1959.47	13099	1	281.4	2.7	-25.4	13537	1	289.9	2.6	-24.5
1959.49	13100	1	290.4	2.8	-25.0	13538	1	292.6	2.8	-24.1
1959.52	13101	1	286.3	2.8	-25.4	13539	1	295.4	2.7	-23.7
1959.54	13102	1	297.4	2.9	-24.2	13540	1	291.4	2.6	-23.6
1959.57	13103	1	296.2	3.2	-24.3	13541	1	290.4	3.0	-23.7
1959.61	13104	1	285.1	4.1	-24.5	13542	1*	256.0	2.6	-24.3
1960.41	13105	1*	254.7	2.3	-25.5	13543	1	224.3	2.8	-25.0
1960.46	13106	1	220.4	2.9	-25.8	13544	1	228.2	2.7	-25.4
1960.47	13107	1	220.3	2.7	-25.8	13545	1	229.4	2.6	-25.0
1960.49	13108	1	228.0	3.5	-25.8	13546	1	233.7	2.6	-24.7
1960.52	13109	1	229.9	3.1	-25.7	13547	1	238.3	2.5	-24.4
1960.54	13110	1	230.0	2.6	-25.1	13548	1	235.0	2.8	-24.1
1960.57	13111	1	232.7	2.7	-24.7	13549	1	239.6	2.7	-24.2
1960.61	13112	1	237.5	2.3	-24.7	13550	1	240.7	2.5	-24.4

463

464

Table S1 continued.

Cellulose midpoint	West cores					East core				
Year (AD)	TRa #	n	$\Delta^{14}C$ (‰)	± (‰)	$\delta^{13}C$ (‰)	TRa #	n	$\Delta^{14}C$ (‰)	± (‰)	$\delta^{13}C$ (‰)
1961.41	13113	1	243.3	3.5	-24.5	13551	1	222.5	2.1	-25.5
1961.46	13114	1	232.8	3.2	-25.0	13552	1	227.3	2.1	-25.9
1961.47	13115	1	233.2	3.7	-25.8	13553	1	224.4	2.4	-25.7
1961.49	13116	1	222.7	2.8	-25.8	13554	1	230.9	2.9	-25.7
1961.52	13117	1	222.0	2.6	-25.9	13555	1	231.0	2.0	-25.1
1961.54	13118	1	229.6	2.2	-25.8	13556	1	235.9	2.2	-25.2
1961.57	13119	1	235.9	2.9	-25.4	13557	1	259.3	2.4	-25.7
1961.61	13120	1	238.2	2.4	-25.3	13558	1*	336.3	2.2	-26.2
1962.41	13121	2*	265.3	4.1	-25.9	13559	1	370.1	2.6	-25.5
1962.46	13122	2*	277.6	4.8	-26.1	13560	1	376.1	2.4	-25.1
1962.47	13123	2	362.7	4.3	-	13561	1	374.3	2.4	-25.0
1962.49	13124	2	370.3	3.7	-	13562	1	414.3	2.7	-25.3
1962.52	13125	2	376.9	4.5	-26.0	13563	1	411.4	2.4	-
1962.54	13126	2	386.4	3.7	-	13564	1	388.1	2.5	-25.1
1962.57	13127	2	392.4	3.5	-25.5	13565	1	422.1	3.0	-25.3
1962.61	13128	2	434.5	4.0	-26.0	13566	1*	516.2	2.9	-
1963.41	13129	2	605.5	3.9	-	-	0	-	-	-
1963.46	13130	2	661.4	4.0	-	13568	1	619.9	5.5	-
1963.47	13131	1	695.4	3.0	-	-	0	-	-	-
1963.49	13132	1	709.7	3.0	-24.6	13570	1	709.0	4.7	-
1963.52	13133	1	751.6	3.0	-	13571	1	754.4	3.3	-24.3
1963.54	13134	1	759.6	3.0	-	13572	1	811.5	3.3	-24.9
1963.57	13135	1	815.8	5.1	-24.3	13573	1	836.8	4.0	-24.6
1963.61	13136	1	831.7	5.1	-24.3	13574	1	869.4	5.1	-25.5
1964.41	13137	1	884.3	3.2	-25.6	13575	1	885.9	4.5	-
1964.46	13138	1	899.7	3.0	-25.4	13576	1	891.7	3.3	-25.5
1964.47	13139	1	898.9	3.6	-	13577	1	906.1	3.2	-25.2
1964.49	13140	1	904.4	5.5	-25.5	13578	1	923.7	4.2	-25.4
1964.52	13141	1	927.8	3.0	-25.6	13579	1	924.8	4.8	-25.2
1964.54	13142	1	927.5	4.4	-25.1	13580	1	922.8	3.3	-24.8
1964.57	13143	1	931.7	2.6	-25.1	13581	1	933.7	3.3	-24.6
1964.61	13144	1	922.6	5.2	-25.0	13582	1*	870.2	3.4	-25.0

Table S1 continued.

Cellulose midpoint	West cores					East core				
Year (AD)	TRa #	n	$\Delta^{14}C$ (‰)	± (‰)	$\delta^{13}C$ (‰)	TRa #	n	$\Delta^{14}C$ (‰)	± (‰)	$\delta^{13}C$ (‰)
1965.41	13145	2*	870.3	5.3	-25.4	13583	1	783.3	3.4	-24.7
1965.46	13146	1	781.4	4.5	-25.8	13584	1	785.8	3.2	-25.4
1965.47	13147	1	782.9	4.4	-25.2	13585	1	786.8	3.8	-
1965.49	13148	1	781.9	4.6	-25.2	13586	1	786.5	3.3	-24.6
1965.52	13149	1	791.2	3.2	-25.1	13587	1	788.9	3.9	-
1965.54	13150	1	792.3	3.7	-24.8	13588	1	787.9	3.7	-
1965.57	13151	1	790.6	2.5	-25.3	13589	1	785.3	2.4	-24.8
1965.61	13152	1	781.1	2.5	-25.0	13590	1*	756.1	2.5	-24.6